APPLICATION OF A MICROMECHANICAL MATERIAL MODEL TO CREEP DAMAGE AND CREEP CRACK GROWTH IN X20 CRMOV 12 1

R. Mohrmann, M. Sester and T. Hollstein*

An 'integrated approach' is proposed as a methodology for predicting the deformation and the lifetime of components operating under creep conditions. This approach is applied to creep crack growth experiments in X20 CrMoV 12 1 at 550°C. Specifically, the Robinson model is chosen for describing visco-plastic deformation and is combined with a model proposed by Rodin and Parks, which models the effect of constrained intergranular cavitation.

INTRODUCTION

Micromechanical material models are a modern tool for modelling the mechanical behaviour of steels and alloys for high-temperature applications. These models have the advantage of having a physical background or being at least motivated by physics. Three main aspects should be distinguished within micromechanical material models, the description of high-temperature deformation, the description of the damaging processes and the interactions of both.

The simple Norton law describes the deformation behaviour by a unique stress/strain-rate relation with no influence of the prior history. In order to model the response to more complex loading and temperature histories, more advanced visco-plastic material models should be used, which are formulated in terms of internal variables representing, for example, kinematic or isotropic hardening phenomena. Visco-plastic material models are appropriate to handle transient mechanical and temperature loading for a calculation of the stress redistribution in pipe

*Fraunhofer-Institut für Werkstoffmechanik, D-79108 Freiburg

bends or for an analysis of the mechanical behaviour of turbine blades under thermal and mechanical loads.

The description of the damaging processes is necessary for the estimation of the lifetime of components. On one hand there are phenomenological models like that of Kachanov, which is based on a formal damage parameter. On the other hand, a micromechanical approach models the physical phenomena such as the nucleation and the growth of pores, the evolution of the carbide structure or the evolution of the subgrain structure. These micromechanical properties may be measured metallographically as well as described with such models.

Deformation and damage may have a strong influence on one another. For example in the case of grain boundary cavitation the strain rate controls whether the cavity growth is constrained or unconstrained. The interactions between deformation and damage should be taken into account choosing an appropriate model. It is recommended to combine both models, which can be done by using the variables for the micromechanical properties as internal variables within the constitutive equations. This is called an 'integrated approach'. The application of such an integrated approach to a component includes the following steps:

- Identification of a model and adjustment of the model parameters to experimental deformation data (creep, relaxation, cyclic loading, ...) and metallographic information.
- Implementation of the material model in a finite element (FE) code.
- FE simulation of the component behaviour.

In the present paper the Robinson model (1), which is capable of describing the high-temperature deformation, is combined with a model developed by Rodin and Parks (2), which models the effect of constrained cavitation on the deformation.

MICROMECHANICAL MATERIAL MODEL

The Robinson model (1) is a visco-plastic material model based on the theory of high-temperature plasticity. It describes isotropic and kinematic hardening but no damaging processes. In an analysis of Rodin and Parks (2) the effect of constrained intergranular cavitation on the stationary creep rate is evaluated. In this analysis an 'acceleration' factor for the stationary creep rate is defined, which models tertiary creep. An empirical equation was chosen for the damage evolution.

Uniaxial formulation. The uniaxial formulation is used for adjusting the model to uniaxial creep data. The equation for the non-elastic strain rate $\dot{\varepsilon}$ has the form:

$$\dot{\varepsilon} = \frac{2A}{\sqrt{3}}\left[\frac{(\sigma-\alpha)^2}{3K} - 1\right]^{n/2} f(\rho,n)\, sgn(\sigma-\alpha) \tag{1}$$

A and n are adjustable material parameters. The back-stress α, the isotropic hardening variable K and the damage parameter ρ are internal variables, which develop according to the following differential equations. Equation (1) is valid if $\sigma(\sigma-\alpha)>0$ as well as $(\sigma-\alpha)^2 > 3K$; otherwise $\dot{\varepsilon}=0$. The function $f(\rho,n)$ models the acceleration of deformation due to constrained cavitation:

$$f(\rho,n) = \left[1 + \frac{2\rho}{n+1} + \frac{(2n+3)\rho^2}{n(n+1)^2} + \frac{(n+3)\rho^3}{9n(n+1)^3} + \frac{(n+3)\rho^4}{108n(n+1)^4}\right]^{(n+1)/2} \tag{2}$$

The evolution laws for the internal variables are

$$\dot{\alpha} = \frac{3}{2}H\left(\frac{|\alpha|}{\sqrt{3}\,\kappa}\right)^{-2\beta} \dot{\varepsilon} / f(\rho,n) - \sqrt{3}R\left(\frac{|\alpha|}{\sqrt{3}\,\kappa}\right)^{2(m-\beta)} sgn(\alpha) \tag{3}$$

$$\dot{K} = \frac{K_s - K_i}{3W_o} e^{-W/W_o} \tag{4}$$

with $\dot{W} = \sigma\,\dot{\varepsilon}$. $H, \kappa, \beta, R, m, K_s, K_i$ and W_O are adjustable parameters, which depend on the temperature. Equation (3) is valid, if $\sigma\alpha > 0$ as well as $|\alpha| > \alpha_o$, with $\alpha_o^2 = 3\kappa^2 G_o$, where G_o is another parameter. Otherwise, in the first term of Eq. (3), α is substituted by α_o. The evolution equation for the damage parameter ρ is taken to be

$$\dot{\rho} = \frac{\rho_f}{\varepsilon_f^{\gamma}}\,\gamma\,|\varepsilon|^{(\gamma-1)}\,\dot{\varepsilon}, \tag{5}$$

with $\rho_f/\varepsilon_f^{\gamma}$ and γ being adjustable parameters. The value of ρ must not be negative. Therefore, the model contains 12 parameters and two initial values for α and K (α_i and K_i, where α_i is set to the value 0 MPa) to describe the nonelastic behaviour. For ρ the definition according to Hutchinson (3) is used. He concluded, that the mechanically relevant damage parameter should be proportional to the number of cavitating facets per volume, N, times their diameter, d, cubed. Specifically he suggested the following form

$$\rho = \frac{n+1}{2(1+3/n)^{1/2}} N d^3 \tag{6}$$

where n is the Norton stress exponent.

Three dimensional formulation. The extension of the model investigated to arbitrary stress states is necessary to enable finite element calculations. The parameters have the same notation and numerical values as in the uniaxial formulation. The tensor of the nonelastic strain rate $\dot{\varepsilon}$ has the form:

$$\dot{\varepsilon}_{ij} = A\left[\frac{J_2(\Sigma_{ij})}{K}-1\right]^{n/2} \frac{\left(1+f(\rho,n)\left(\sigma_I/\sigma_e\right)^2\right)^{(n-1)/2}}{\sqrt{J_2(\Sigma_{ij})}} \left(\Sigma_{ij}+\frac{2}{3} f(\rho,n)\,\sigma_I \frac{\partial \sigma_I}{\partial \sigma_{ij}}\right) \tag{7}$$

J_2 denotes the second invariant of the effective stress Σ, where $\Sigma=\mathbf{s}-\alpha$ is the difference between the deviator of the stress tensor $\mathbf{s}$, and the back-stress tensor α, which is deviatoric by definition. The back-stress tensor α, the isotropic hardening variable K and the damage parameter ρ are internal variables, which develop as given in the following differential equations. The function $f(\rho,n)$ and the evolution for K are given in equations (5) and (4), respectively; σ_I and σ_e denote the maximum principal and the v.Mises equivalent stress, respectively. Equation (7) is valid if $\mathbf{s}\Sigma > 0$ as well as $J_2(\Sigma) > K$, otherwise $\dot{\varepsilon}=0$. The evolution laws for the internal variable α is

$$\dot{\alpha}_{ij} = AHG^{-\beta}\left[\frac{J_2(\Sigma_{ij})}{K}-1\right]^{n/2} \frac{\Sigma_{ij}}{\sqrt{J_2(\Sigma_{ij})}} - RG^{m-\beta} \frac{\alpha_{ij}}{\sqrt{J_2(\alpha_{ij})}}. \tag{8}$$

Equation (8) is valid, if $\Sigma\alpha > 0$ as well as $G > G_o$, with $G = J_2(\alpha)/\kappa^2$, where G_o is another parameter. Otherwise, in the first term of Eq. (8), G is substituted by G_o. The evolution equation for the damage parameter ρ is

$$\dot{\rho} = \frac{\rho_f}{\varepsilon_f^{\gamma}} \gamma \left(\frac{2}{3}\varepsilon_{ij}\varepsilon_{ij}\right)^{(\gamma-1)/2} \left(\frac{2}{3}\dot{\varepsilon}_{ij}\dot{\varepsilon}_{ij}\right)^{1/2} \frac{\sigma_I}{\sigma_e} \tag{9}$$

with the parameters $\rho_f/\varepsilon_f^{\gamma}$ and γ. This formulation allows ρ to shrink under compression, therefore there is no net damage for symmetric cyclic loading.

Finally, the coupling of the stress rates and the strain rates is given by the differentially formulated Hooke's law

$$\dot{\sigma}_{ij} = E_{ijkl}\left(\dot{\varepsilon}_{kl}^{tot} - \dot{\varepsilon}_{kl}\right) \tag{10}$$

where $\boldsymbol{E}$ and $\dot{\varepsilon}^{tot}$ are the tensor of elastic moduli and the total strain rate tensor, respectively.

MODELLING OF CREEP DATA

Optimisation method. Constitutive equations with internal variables cannot generally be integrated in closed form to give, for example, creep or relaxation curves. Hence, a program system must be applied that allows the numerical integration of the constitutive equations for arbitrary testing conditions (constant load, constant stress, constant strain rate, relaxation, cyclic loading, etc.). The integration routine is a subprogram of a program that varies the parameters of the constitutive equations in such a way that the deviation from experimental data (for example, in terms of chi-square) is minimal. The aim is to optimise the parameters in relation to a whole set of experiments including creep tests at various stresses and other types of tests. For the present paper, however, only creep tests were available to which the model could be adjusted.

Adjustment of parameters. The model has been applied to the 12%-chromium steel X20 CrMoV 12 1. The deformation was modelled based on the creep data of nine creep tests performed at 550°C. These tests are constant load tests with a duration of up to 30 000 h. Primary, secondary and tertiary creep behaviour could be observed. The uniaxial formulation of the model, which is capable of describing isotropic and kinematic hardening as well as constrained cavitation, was adjusted to the primary, secondary and tertiary part of the creep curves, i.e. the 13 model parameters were optimised simultaneously with respect to all nine creep curves. For this optimisation a self-developed software package called 'Fitit' was used.

Results. The optimised parameter set is given in Table 1. The agreement between the model investigated, denoted with 'Robinson model with damage', and the creep curves is satisfactory: In Figure 1 the creep data and the modelling result are plotted

TABLE 1. Optimised Parameter Set.

A	n	H	κ	β	R	
$3.55\ 10^{-15}$	9.00	$3.11\ 10^{+6}$	$1/\sqrt{3}$ fixed	.853	$8.49\ 10^{-8}$	
m	G_o	K_S	W_o	K_i	γ	$\rho_f / \varepsilon_f^{\gamma}$
1.02	859.	549.	.124	66.4	1.41	173.

units in MPa, sec

with a log strain rate scale over a log strain scale. The strain rate values are calculated according to a two point differential quotient. This formula produces large scatter for low strain rates. Therefore experimental data points with strain rates below 10^{-4} %/h are omitted from Fig. 1. Figure 2 shows the strain versus normalised time for three creep tests. The stress dependence of the strain ratio (i.e. fracture strain divided by Monkman-Grant product) for different stress levels can be calculated from the experimental data and is described by the model investigated.

PREDICTION OF INDEPENDENT EXPERIMENTS

Creep crack growth experiments with side grooved compact tension (CT) specimens (geometry B/W = 20/50) made of X20 CrMoV 12 1 were performed at different load levels at 550°C (4). In these experiments, the load line displacement was measured on-line and, in addition, the crack extension was determined after the specimen had been fractured at RT.

Finite Element Implementation. In order to predict these experiments with the help of the combined Robinson and Rodin and Parks model, the three dimensional form of the constitutive equations (7)-(10) was implemented by writing a user material subroutine UMAT for the FE code ABAQUS. ABAQUS provides kinematical quantities (total strain increments or deformation gradients) and the user has to perform the integration of the constitutive equations on the element level yielding the updated stress in the global balance of momentum equations. The system of differential equations (7)-(10) can behave mathematically very 'stiff' in the sense that roundoff errors grow exponentially, thus requiring special care in choosing suitable integration schemes. In our implementation, the numerical integration is done by a stepsize-controlled fourth order Runge-Kutta scheme. An accurate and stable integration is accomplished by subincrementing the global time step in such a way that an estimate of the local truncation error of a single Runge-Kutta step is within prescribed bounds. At the time of submitting the manuscript, the implementation of the complete set of equations (7)-(10) was not yet finished. In this paper, results of simulations are presented in which the effect of damage on the deformation behaviour is neglected ($\rho \equiv 0$ in eqn. (7)) and eqn. (9) is evaluated by post processing the FE results.

Results and Discussion. Four experiments were simulated with finite elements, employing the Robinson model without damage. One representative quarter of a CT specimen was modelled with 450 three dimensional 20 noded solid elements. The mesh is shown in Figure 3 where the ligament is shaded and the loading point is marked by an arrow. The CPU times ranged from 3 hours up to 10 hours on an engineering workstation. Figure 4 shows a comparison of the measured and calculated load line displacements in the four experiments. The agreement is good. This holds especially for the experiments undergoing only little creep crack growth (F=6200 N and F=9800 N). Since damage evolution and crack growth were not

modelled, the poorer agreement for the higher loads, where more crack growth occurred, is not surprising.

Of course, the FE mesh is too coarse to give an accurate description of the crack tip fields. Note that the side lengths of the crack tip elements are just in the range of the depth of the side groove. Nevertheless, for a qualitative assessment, the distribution of the field variables in the vicinity of the crack tip is given. The relaxation of the v. Mises stress due to creep is shown in Figs. 5 to 7. Figure 8 gives the ratio of the maximum principal stress to the v. Mises stress, which has a substantial impact on the creep rate in the Rodin and Parks model. Figures 9 and 10 show the distribution of the damage parameter at t = 10 h and t = 1000 h obtained by post processing the FE results. At t = 1000 h a heavily damaged zone with $\rho > 2.5$ spreads about 0.7 mm into the ligament. Clearly, in a fully coupled deformation and damage analysis with the complete set of equations (7)-(10), this amount of damage would have a strong effect on the crack tip stress and strain fields and thus on the rate of damage evolution itself. In the corresponding experiment, the measured creep crack growth was about two times larger than the extension of the heavily damaged zone predicted by the uncoupled analysis.

CONCLUSION

The numerical tools for the application of micromechanical material models are developed. The application to CT-specimens shows a reasonable agreement between the prediction and the experiment. The numerical effort of the calculations does not exceed the capacity of a workstation. Therefore this method may be used for more extended applications like real components.

We acknowledge many fruitful discussions with Dr. H. Riedel.

REFERENCES

(1) D. N. Robinson, A Unified Creep-Plasticity Model for Structural Metals at High Temperature, ORNL Report/TM-5969 (1978).

(2) G. J. Rodin and D. M. Parks, J. Mech. Phys. Solids **36** (1988) 237-249.

(3) J. W. Hutchinson, Acta metall. **31** (1983) 1079-1088.

(4) M. Sester, R. Mohrmann, H. Riedel und T.Hollstein, Entwicklung von mikromechanischen Materialmodellen zur Beschreibung von Kriechschädigung, IWM-Report Z7/93, Freiburg (1993).

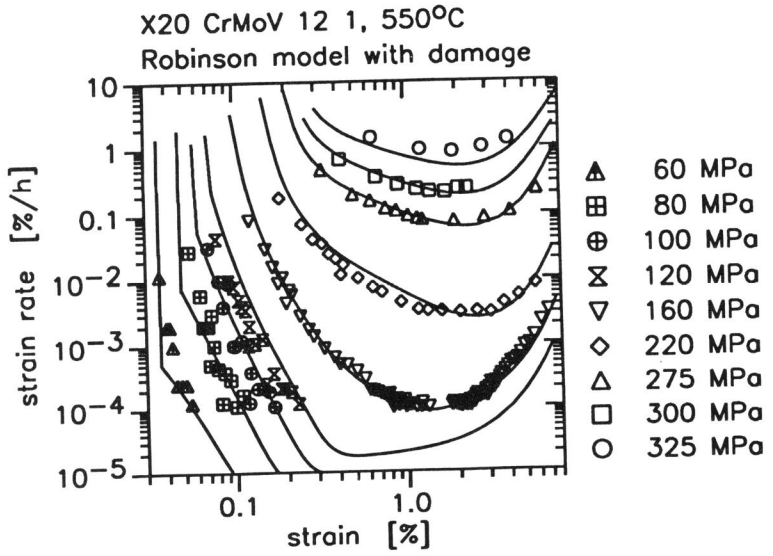

Figure 1: Creep data for X20 CrMoV 12 1 at 550°C and modelling results.

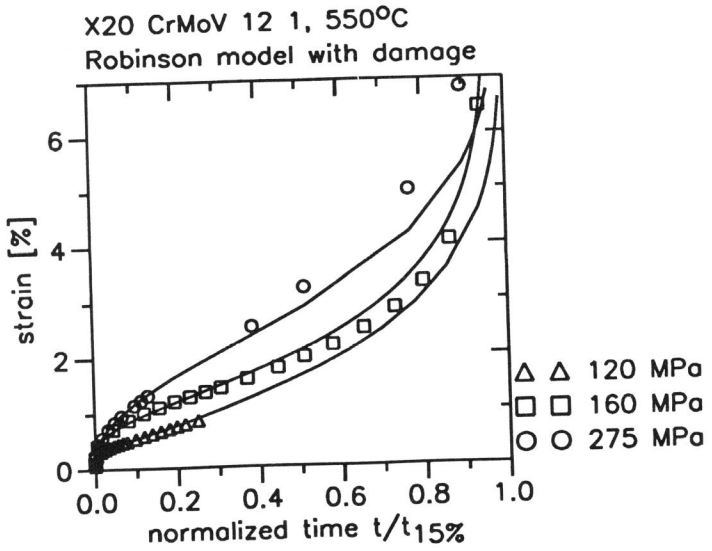

Figure 2: Creep curves for X20 CrMoV 12 1 at three stress levels.

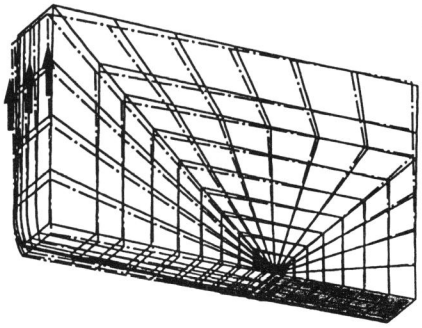

Figure 3: Original and displaced mesh of a CT specimen.

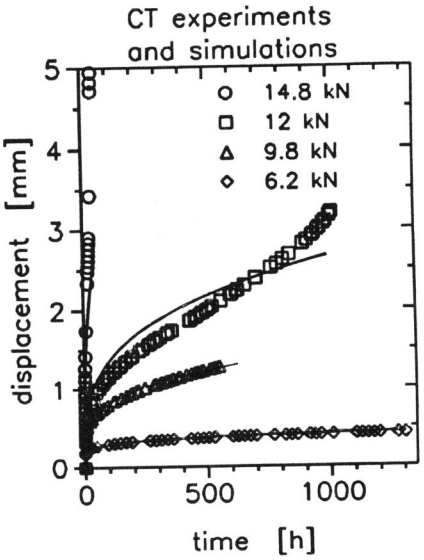

Figure 4: Load line displacement: measurements (symbols) and simulations.

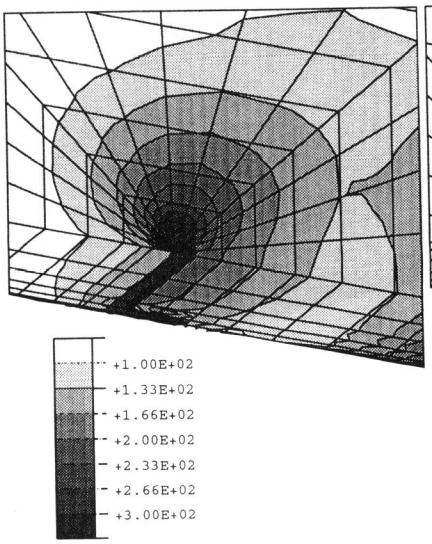

Figure 5: V. Mises stress distribution at t = 0.03 h.

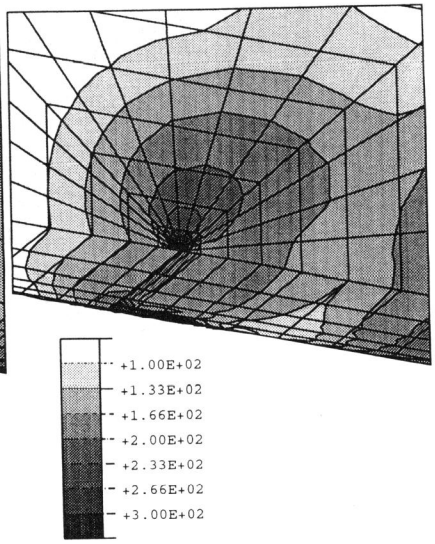

Figure 6: V. Mises stress distribution at t = 10 h.

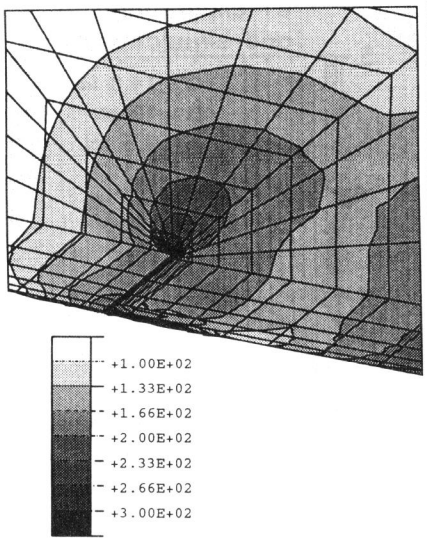

Figure 7: V. Mises stress distribution at t = 1000 h.

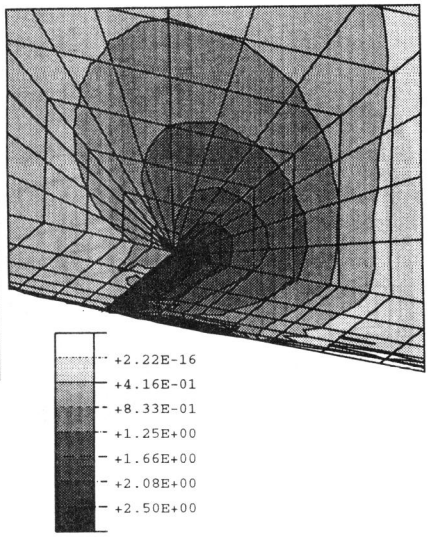

Figure 8: Ratio of maximum principal stress to v. Mises stress at t = 1000 h.

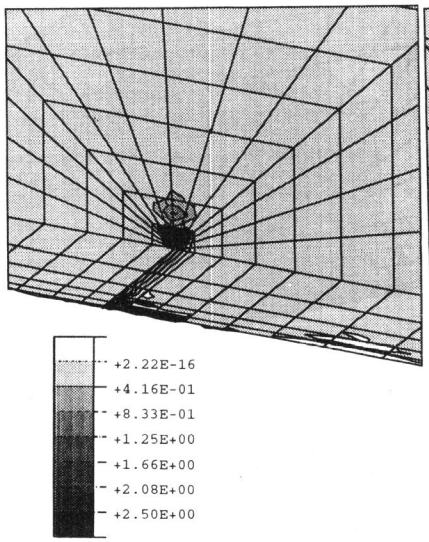

Figure 9: Distribution of the damage parameter at t = 10 h.

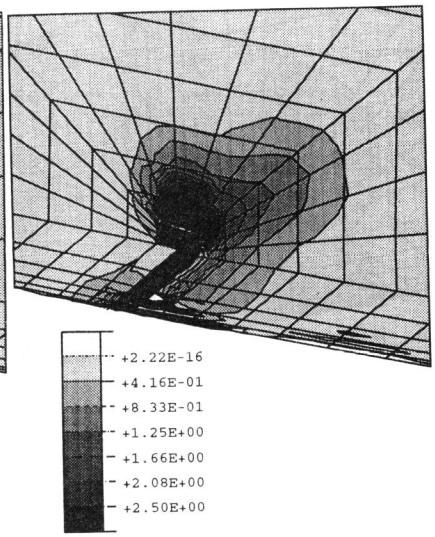

Figure 10: Distribution of the damage parameter at t = 1000 h.